EPJ Web of Conferences **346**, 01030 (2026) https://doi.org/10.1051/epjconf/202634601030
RFPPC2025

The present status of the TORIC-SSFPQL codes

Marco Brambilla[1,*] and *Roberto* Bilato[1,**]

[1]Max Plank Institute for Plasma Physics, Boltzmannstr. 2, D 75748 Garching, Germany

Abstract. The codes TORIC and SSFPQL allow detailed selfconsistent simulations of wave propagation and absorption in the Ion Cyclotron (IC) range of frequencies in tokamak plasmas. We review the options presently available in the codes, and we illustrate their performances with two examples: a typical minority heating experiment in a medium size device, and a possible IC heating scenario in a ITER like plasma. The problem of ensuring charge neutrality when the ion distribution functions develop anisotropic suprathermal tails is discussed.

1 Introduction

The codes TORIC [1] and SSFPQL [2] have been developed into a "user-friendly" package, which allows detailed simulations of auxiliary heating scenarios in the Ion Cyclotron (IC) range of frequencies in tokamaks, with very moderate CPU memory and time requirements. TORIC solves Maxwell's equations using the spectral method in the toroidal and poloidal angles, and cubic Finite Elements in the radial coordinate. The coefficient of the wave equations are evaluated on each magnetic surface using the quasilinear (QL) ion distribution functions (IDFs) obtained from SSFPQL [3]. By exploiting the axisymmetry in tokamaks, the wave equations are solved separately for each toroidal Fourier mode (these runs can be executed in parallel), and the results for the individual modes are superposed with the weights determined by the antenna geometry and feeding. In turn, SSFPQL solves the steady-state kinetic equation normalizing the QL diffusion coefficient $D_{\rm QL}$ using the power deposition profiles obtained by TORIC. The solutions for each ion species on each magnetic surface are obtained by expanding the IDFs in Legendre polynomials in the cosine of the velocity pitch angle; a special Bessel function identity in the Legendre representation of $D_{\rm QL}$ [2] avoids the convergence problems which plague the power expansion in the Larmor radius originally proposed for this purpose [4]. The iteration to reach consistency between TORIC and SSFPQL is executed automatically by specifying a few parameters in the namelists [5].

The Grad-Shafranov MHD configuration (in the inverse Fourier representation [6]) and the measured density and temperature profiles are read from external files in standardized format; alternatively, simple analytic approximate equilbria and plasma profiles can be used. In TORIC it is possible to take into account all Large Larmor Radius corrections to the coefficients of the wave equations necessary to the description of electron Landau damping (ELD) of Ion Bernstein waves and ion heating at higher IC harmonics. In SSFPQL we have implemented the QL diffusion coefficient $D_{\rm QL}$ derived by Catto and Myra [7, 8], which takes into account the effects of toroidal trapping on the QL IDFs. To simulate the synergy between hf heating and Neutral Beam Injection (NBI), the code SINBAD [9],has been added to the package [10, 11]. A dedicated modulus calculates the distribution of thermonuclear alpha particles in slowing down [12] and their contributions to the coefficients of the wave equations [13, 14]. A set of auxiliary routines is available for the preliminary investigation of each scenario (position of resonances and cutoffs, local dispersion relation), including an adapted version of the FELICE code [15] for detailed study of the IC antenna.

Sections 2 and 3 presents two example of applications of the codes, respectively for minority heating in a medium-size tokamak, and for an auxiliary heating scenario in ITER. In section 4 we discuss the charge neutrality problem which arises when the QL IDFs are evaluated taking toroidal trapping into account [16, 17], and we present the solution proposed for SSFPQL.

2 Simulation of a minority heating scenario in ASDEX Upgrade

We illustrate the use of the codes for a typical minority heating experiment in ASDEX Upgrade (AUG): 3% Hydrogen in a Deuterium plasma with central parameters $n_e(0) = 5.94\ 10^{19}\ {\rm m}^{-3}$, $T_e(0) = 4.19$ keV, $T_i(0) = 4.67$ keV, B(0) = 2.5 Tesla. We have assumed 4 MW at 36.5 MHz coupled to the plasma, with the fundamental IC resonance of Hydrogen and first IC harmonic of Deuterium located a couple of cm on the low field side of the magnetic axis. A poloidal cross-section with the resonance and cutoff location is shown in fig. 1, and information on the local dispersion relation along the equatorial plane in fig. 2.

*Corresponding author: Marco.Brambilla@ipp.mpg.de
**Corresponding author: Roberto.bilato@ipp.mpg.de

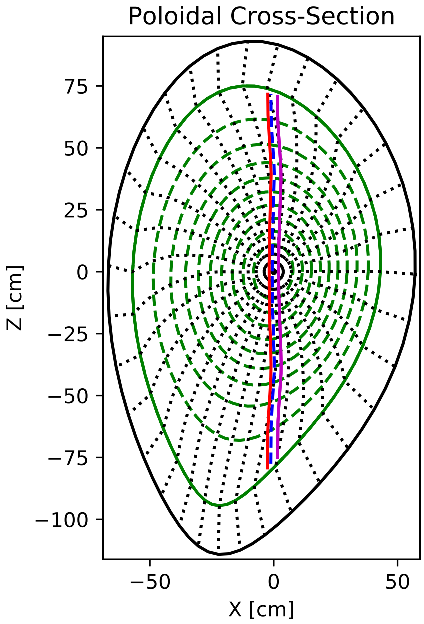

Figure 1. Poloidal cross-section of ASDEX Upgrade equilibrium, with with the coordinate lines, and with IC resonances (violet), ion-ion resonances (red) cutoffs (blue). The full green curve is the plasma boundary, and the full black curve the vessel assumed by TORIC.

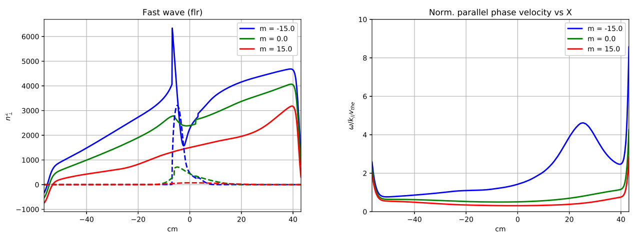

Figure 2. Left: perpendicular index squared of the Compressional wave along the equatorial plane, for the toroidal mode $n_\varphi = 20$. Right: $\omega/k_\parallel v_{the}$ along the equatorial plane for the toroidal mode $n_\varphi = 20$, illustrating the variation of absorption by the electrons, depending on the poloidal wavenumber m.

The toroidal power spectrum from the 3-strap IC antenna of AUG [18] evaluated by TORIC is shown in fig. 3; it is similar to, but somewhat more irregular than the spectrum calculated by FELICE imposing outwards radiation conditions just outside the near field region [1]. Note that the TORIC and FELICE spectra are somewhat different around $n_\varphi = 0$. This is because to fully exploit axisymmetry TORIC assumes the current distribution in the antenna to be factorized into a function of the poloidal angle describing the current along the straps, times a function of the toroidal angle describing the position and phases of the straps. The 3-strap antenna of AUG does not satisfy this condition exactly, and FELICE, in contrast to TORIC, can take this into account.

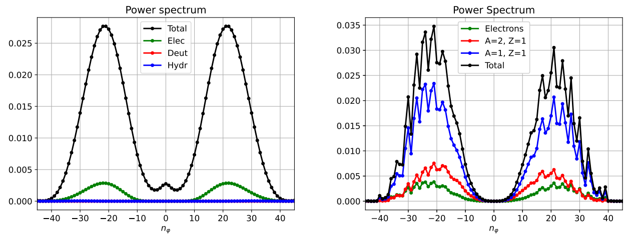

Figure 3. Left: Toroidal power spectrum from the 3-strap IC antenna of ASDEX Upgrade according to FELICE, with outwards radiation conditions imposed just outside the near field domain. Right: the same spectrum according to TORIC. The left-right asymmetry is due to the poloidal component of the static magnetic field.

In the core of a medium size tokamak the hf power density can reach several Watt/cm^3. Under these conditions the heating rates predicted by TORIC and SSFPQL for a Maxwellian plasma differ substantially (cf. fig 4, left) and five or more iterations are needed to reach agreement between the two codes. In principle, at each iteration the QL diffusion coefficient in SSFPQL should include the contributions of all toroidal modes radiated by the antenna (this option is used in our examples). However, since the results of TORIC vary only slowly with n_φ, one can accelerate the computation by taking into account only a selection of modes, for example one every five. A reasonable approximation can even be obtained by performing the loop for a single representative toroidal mode, chosen at the peak of the antenna spectrum.

After integrating the QL kinetic equation, on each magnetic surface SSFPQL evaluates the QL Plasma Dispersion Functions (PDFs), defined for species i and real argument as

$$\tilde{Z}_i(x_p) = P\int_{-\infty}^{+\infty} \frac{\tilde{F}_i(u)}{u - x_p}\mathrm{d}u + i\pi\tilde{F}_i^p(x_p) \qquad x_p = \frac{\omega - p\Omega_{ci}}{k_\parallel v_{thi}} \tag{1}$$

with

$$\tilde{F}_i^p(u) = \int_0^\infty F_i(u, w)\, w^{2p-1}\,\mathrm{d}w. \tag{2}$$

Here F_i is the QL ion distribution function obtained from SSFPQL, normalized to unity, $u = v_\parallel/v_{\rm thi}$, $w = v_\perp/v_{\rm thi}$, with $v_{\rm thi}$ any convenient average speed (the thermal speed if F_i is Maxwellian; in this case $\tilde{Z}$ reduces to the usual PDF). An efficient routine has been written to perform the Hilbert transform in eqn (1) [19]. Since the QL diffusion coefficient used is bounce-averaged, the IDF in the integrand of (1) is evaluated by SSFPQL at the outer equatorial point of each magnetic surface, and is "mapped" to the resonance position. To maintain charge neutrality, it is assumed that the trapped ions turning before reaching the resonance are replaced there by the appropriate number of thermal ions (cf. section 3).

After each iteration the absolute difference of the heating rates predicted by TORIC and by SSFPQL is integrated over the whole plasma, and the iteration is stopped

[1] FELICE can solve wave equations over either the entire plasma column with metallic reflection at the opposite wall or a finite region under the antenna with an arbitrary thickness and outward radiation conditions at the far boundary. As the plane-stratified geometry significantly overestimates the quality factor of potential internal modes due to reflected waves, the latter option — with the boundary positioned prior to any singularity in the wave equations — provides the most accurate modeling of the radiated spectrum and the antenna load.

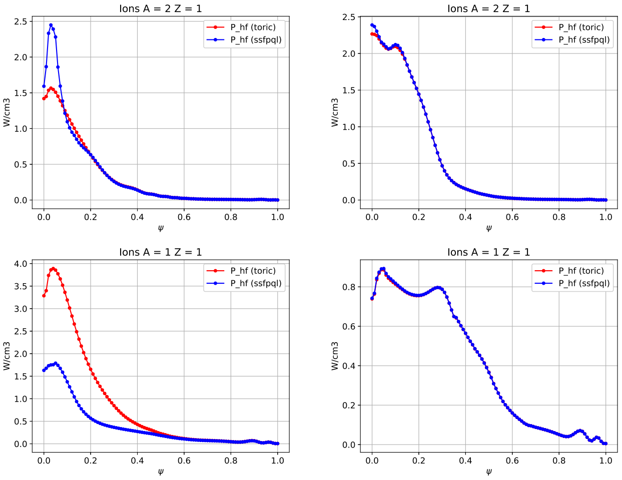

Figure 4. Power deposition profiles predicted by TORIC (blue) and SSFPQL (red). Left: Maxwellian plasma, right': at convergence. Above: Deuterium, below: Hydrogen.

when the result is less than an 'accuracy goal' prescribed by the user (in the present example 0.5% of the total hf power, i.e. 20 kW versus 4 MW). The 'history' of the loop is shown in fig. 5. As the suprathermal populations develop, direct absorption by Deuterium increases, in agreement with the fact that IC harmonic heating is a finite pressure effect. Direct absorption by the minority decreases, and collisional transfer to the electrons by suprathermal protons also decreases somewhat. Note that this is not a time history, although the results of TORIC at the initial iteration, in which the IDFs are assumed to be Maxwellians, can be regarded as the performance at the start of the heating pulse, when the plasma is still in local thermal equilibrium.

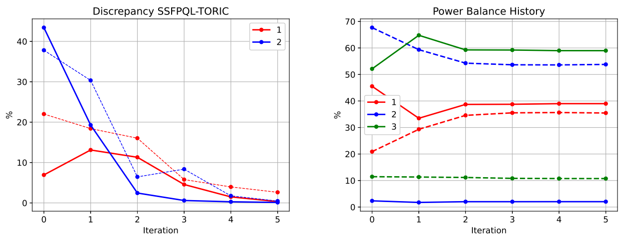

Figure 5. History of the consistency loop. Left: Discrepancy between the predictions of TORIC and SSFPQL. Right: predicted global power balance at each iteration (red: Deuterium; blue: Hydrogen; green: electrons; dashed lines: fraction of the available hf power absorbed from the waves; full curves: fraction of the power in each species after collisional relaxation)

The power deposition profiles predicted by the two codes in the Maxwellian plasma and at convergence are shown in figs. 4 (note the different vertical scales). The importance of performing the iterations is clearly illustrated by these figures. For the Maxwellian plasma, as soon as the local power absorption exceeds a few tens of Watt/cm^3 SSFPQL predicts a much lower heating rate than TORIC, especially for the Hydrogen minority. More important, the profiles predicted at convergence, when the two codes use the same QL IDFs to calculate the heating rates on all magnetic surfaces, are quite different from those predicted by TORIC for the Maxwellian plasma. In the core, the hf power per cm^3 absorbed by Deuterium is 1.6 times higher than in the Maxwellian plasma, again in agreement with the fact that IC harmonic heating is a finite pressure effect. Core absorption per cm^3 by the Hydrogen, by contrast, is almost four times lower; globally, however, this is almost entirely compensated by a marked broadening of the profile, due to the increased Doppler broadening by the suprathermal tail.

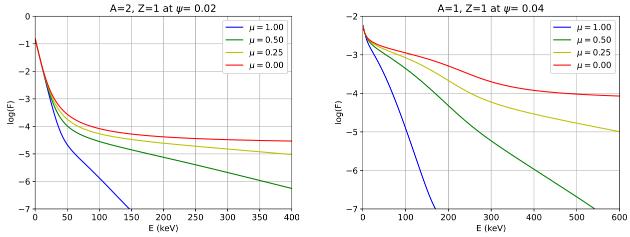

Figure 6. Log plots of the quasilinear distribution functions of Deuterium (left) and Hydrogen (right) at the point of maximum power absorption, at convergence. The curves are for different values of μ.

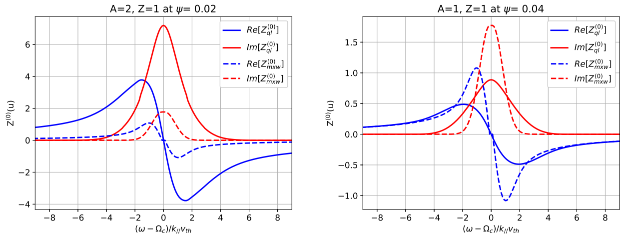

Figure 7. Comparison of the QL Plasma dispersion functions (full curves) with the Plasma dispersion functions of the Maxwellian plasma (dashed curves) Deuterium left) and Hydrogen (right) at the point of maximum power absorption.

The selfconsistent QL IDF $F_i(v,\mu)$ ($\mu = v_\parallel/v$) of Deuterium and Hydrogen are shown in fig. 6, and the corresponding QL Plasma Dispersion Functions $-x_0\tilde{Z}_i(x_p)$ (QL PDF) at the point of peak absorption in fig. 7[2]. Note that the imaginary part of the QL PDF of the Deuterium is not only broader, but also larger in absolute value with respect to the Maxwellian PDF: this is again a result of the fact that absorption at the IC harmonic is proportional to the pressure of the heated species. By contrast, the imaginary part of the QL PDF of Hydrogen is broadened by the increased Doppler effect, but encloses always the same area: IC heating at the fundamental is a Zero Larmor Radius effect.

To complete the example, we have repeated the consistency loop assuming that 4.86 MW of Deuterium NBI

[2]The QL PDF are plotted for convenience at the point of maximum power absorption, but are calculated by SSFPQL and transmitted to TORIC at the IC resonance of all magnetic surfaces of the radial mesh, 100 radial points in the present example. They are then interpolated on the finer radial mesh of TORIC, in the examples 501 radial point. In the poloidal angle 64 points, corresponding to 31 poloidal Fourier modes were used.

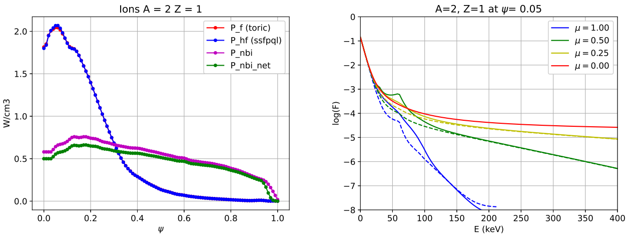

Figure 8. Left: Power deposition profiles in Deuterium with 4.86 MW of NBI. Right: Log plots of the quasilinear distribution functions of Deuterium at the point of maximum power absorption, at convergence. Full lines: NBI direction; dashed line: opposite direction.

where also present. The NBI power deposition profiles are calculated by the version of the code SINBAD [9], included in the TORIC-SSFPQL package [11], using the geometry of the NBI injectors of AUG. The results at convergence are shown in fig. 8.

3 An Ion Cyclotron heating scenario in ITER

In reactor-grade plasmas, such as ITER, the hf power available per ion will be at least one order of magnitude smaller than in present day experiments, and probably even smaller. As a consequence, the difference between the Maxwellian and the selfconsistent QL simulation is much smaller, and one or two iterations are sufficient to reach agreement between TORIC and SSFPQL. We present a set of simulations of a IC heating scenario using ^{3}He minority, with increasing background temperatures, illustrating the effects on the IC power deposition profiles of the increasing competition from absorption by the electrons, and in certain situations also from the increasing population of thermonuclear alphas in slowing down.

As ‘catalyst’ for efficient IC heating in ITER it has been proposed to inject a small quantity of Helium 3. The chosen concentration must be a compromise between the high cost of this gas, and the requirement that a substantial fraction of the hf power absorbed by the minority should be transferred collisionally to the ions. In our simulations ^{3}He was assumed to have a concentration of 3% in a D-T plasma in equal concentrations [20]. With a magnetic field on axis of 5.3 Tesla and an applied frequency of 52.5 MHz the fundamental of ^{3}He (and the first harmonic of Tritium) was located a few cm on the low field side of the magnetic axis. For the simulations we have used a numerically calculated equilibrium, and analytic density and temperature profiles, varying the central temperature from 4 keV (Ohmic plasma) to 20 keV (roughly ignition). The central density was kept constant at $n_e = 1.05\,10^{20}$ m^{-3}. In this way, of course, there is no consistency between the pressure profiles and the numerical Grad-Shafranov equilibrium, which is kept constant while varying the temperature, and thus pressure. A further limitation is that the accumulation of ashes (thermalized alpha particles) has been evaluated with a purely heuristic model, arbitrarily assuming that their concentration on axis reaches 5% in number at 20 keV, and is otherwise proportional to the local electron density multiplied by the local concentration of thermonuclear alphas in slowing down. The concentration and distribution function of the latter, on the other hand, is calculated at each magnetic surface solving the appropriate kinetic equation, and is very close to the analytic distribution [12], except near the thermal region. In the present scenario, however, the alpha particles do not absorb a significant fraction of the hf power, since very little power reaches their fundamental IC resonance (and of the Deuterium) located almost 150 cm to the high field side of the magnetic axis. Competition for hf power with ^{3}He comes from Tritium, and at high temperature mainly from the electrons.

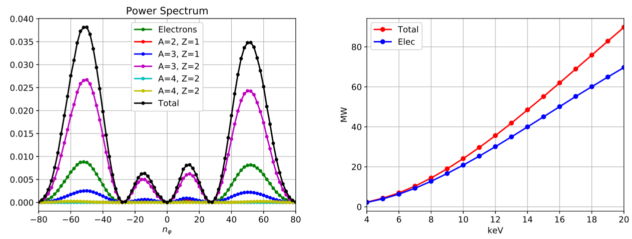

Figure 9. Left: Toroidal power spectrum of the antenna proposed for ITER [21]. The power repartition between different species is for a central temperature of 15 keV. Right: Plasma heating rate from thermonuclear α particles in slowing down, as function of the plasma central temperature. Red: total; Blue: fraction going to the electrons.

The power spectrum of the antenna proposed for ITER [21] predicted by TORIC is shown in fig. 9, left. Because absorption is almost complete in a single pass, in this case the spectrum is almost identical to the one calculated by FELICE. The shape of the total radiated power spectrum is insensitive to the plasma temperature; in fig. 9, on the other hand, the repartition of the hf power among species is that at the central temperature of 15 keV.

We have explored how this IC heating scenario is affected by the increasing plasma temperature as ignition is approached. In this exploration the temperature is varied as a parameter: a transport code for the consistent time evolution of the discharge in the presence of both thermonuclear alphas and hf heating is not available in the TORIC-SSFPQL package. As a further unrealistic assumption, we have performed the consistency loops between TORIC and SSFPQL for a total hf power of 40 MW, much higher than the power effectively planned at least for the initial phase of ITER. We think that 40 MW is the minimum hf power which has some chance of contributing to bring the plasma from the Ohmic state towards ignition. As shown in fig. 9 right, the heating rate of the plasma by thermonuclear α particles in slowing down exceeds 40 MW already at the central temperature of 13 keV. In view of these limitations, we have performed the temperature scan for the representative toroidal mode $n_\varphi = 50$ only, rather than for the entire toroidal spectrum. Clearly, our results are only indicative; nevertheless the trends ob-

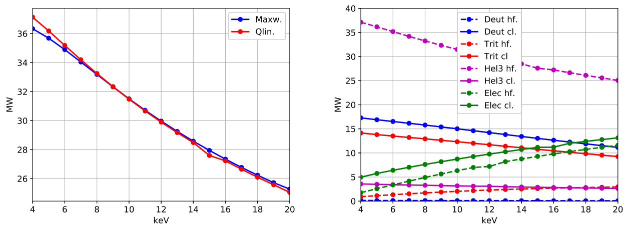

Figure 10. Left: Fraction of the hf power absorbed by the ^{3}He minority in the Maxwellian plasma (blue) and in the consistent QL situation (red) as a function of the central temperature. Right:Hf power going to ^{3}He, Tritium, and Electrons in the consistent QL situation as a function of the central temperature. Dashed curves: direct absorption; full curves: after collisional equilibration.

tained reflect the real situation, and are sufficiently interesting to deserve being reported.

Even at 40 MW total power, the power per ions is so small that the consistency loops between TORIC and SSFPQL converge in one or two iterations, and the difference between the predictions of TORIC for the Maxwellian plasma and the results in the consistent QL situation are much smaller than in the previous case. As an example, this difference is shown for the global absorption by ^{3}He in fig. 10 left.

Figure 10 right shows the hf power going to the different charged species, directly from hf absorption (dashed lines), and after collisional equilibration (full lines). In the Ohmic plasma more than 90% of the hf power is absorbed by the ^{3}He minority; this fraction decreases to less than two thirds at 20 keV. As anticipated, above 10 keV competition is mainly from the electrons, which in the region between the outer plasma edge and the IC resonance of ^{3}He absorbs a fraction of the total power increasing from less that 5% at 4 keV to almost one third at 20 keV. Some competition comes also from Tritium: since heating at the first harmonic is a finite pressure effect, the fraction absorbed by Tritium, in spite of the increasing electron damping, increases from 2.3% at 4 keV to 7.4% at 20 keV. It is also worth mentioning that at the highest temperatures about 0.3 MW are absorbed by the thermonuclear α particles, in spite of the unfavourable position of their IC resonance. In scenarios where this resonance is directly exposed to the incoming power, thermonuclear αs can absorb a substantial fraction of the available hf power. We recall that in TORIC the evaluation of absorption by high energy alphas takes into account that their Larmor radius in the high energy part of their energy spectrum is of the same order as the wavelength of the compressional wave.

After collisional redistribution, in the Ohmic plasma somewhat more than 40% of the hf power is found in the Deuterium, and 35% in the Tritium; only 5% is deposited in the electrons. The fraction in the electrons increases with temperature, reaching one third at 20 keV. As mentioned above, because of the cost of ^{3}He, it is considered preferable to reduce the concentration of this minority to 2% or perhaps even 1%. This scenario is rather sensitive to the ^{3}He concentration: as $n_{^3\mathrm{He}}/n_e$ decreases, the hf power directly absorbed by the ^{3}He decreases, while the fraction thereof collisionally transferred to the electrons increases. Although these two effects in part compensate each other, the net result is an increase of the hf power finally deposited in the electrons. According to TORIC-SSFPQL, at the central temperature of 5 keV, direct absorption by the ^{3}He is 92% at the concentration of 3%, 88% at the concentration of 2%, and 78% at the concentration of 1% in number. At the same time, the fraction of the total hf power finally going to the electrons increases from 14% to 17% and to 24%; this power adds to the already large power deposited in the electrons by the thermonuclear α particles. Hence a compromise must be found between economy of cost, and efficiency in transferring the hf power preferentially to the ions. In fact, the plan is to introduce ^{3}He in the initial phase of the discharge and allow it to diffuse as the temperature rises towards ignition. As we lack a model of ^{3}He transport, we have kept the concentration constant. Therefore, our results only illustrate how TORIC-SSFPQL could be used in this context.

4 Implementation of toroidal trapping in SSFPQL and the mapping problem

The effects of toroidal trapping on the development of the strongly anisotropic suprathermal populations produced by IC heating have been included in SSFPQL [8] by implementing the QL diffusion coefficient proposed by Catto and Myra [7]. Compared to the case in which toroidal trapping is ignored, the Catto-Myra diffusion coefficient is appreciably larger near the magnetic surface tangent to the IC resonance, and decreases more rapidly away from this surface [22]. This has a visible effect on the power deposition profiles predicted by SSFPQL for the Maxwellian plasma, particularly in the case of the Deuterium. Remarkably, however, it turns out that the consistent absorption profiles are practically identical to those predicted ignoring trapping. This appears to be true in general: the converged profiles are surprisingly insensitive to the detailed model used to build the QL diffusion coefficient.

Since the Catto-Myra diffusion coefficient is bounce-averaged, the QL IDFs in the integrand of eqn (1) are evaluated by SSFPQL at the outer equatorial point of each magnetic surface. To evaluate IC absorption, however, TORIC needs the QL PDFs at the points where the magnetic surface cuts the IC resonance. As mentioned above, therefore, the IDFs must be “mapped” to the resonance position. This raises a seldom mentioned problem in modeling of wave propagation in ion cyclotron range of frequencies (ICRF), namely preservation of charge neutrality [23]. Because of toroidal trapping, not all ions present at the outer equatorial point reach the resonance: in particular, IC heating tends to accumulate energetic ions on trapped orbit which barely miss the resonance (this feature of the QL distribution function is known as ‘rabbits ears’ in the literature). Trapped ions with turning point on the low field side of the resonance are not, or very little, heated, and this has to be taken into account when evaluating the QL PDFs to be used by TORIC to evaluate IC damping.

The fact that a non-neglegible number of ions are reflected before reaching resonance means that, when the ion distribution function develops anisotropy and the mapping is performed using the constancy of energy and momentum, the ion density is no longer constant on the magnetic surface. With power absorption densities of the order of Watts/cm^3, the amplitude of the ion density variations associated to the QL IDFs calculated by SSFPQL can reach several percent of the local electron density, manifestly a physically unacceptable result.

In the real plasma, of course, an ambipolar potential $\Phi(\psi, \vartheta)$ varying with the poloidal angle will develop in order to maintain charge neutrality. Taking this potential consistently into account is difficult: the neutrality condition determining the potential is non linear, and could be imposed only by iterating SSFPQL, since initially neither the distribution functions nor Φ itself are known. This, in turn, is made next to impossible by the fact that the effects of Φ on the unperturbed ion orbits have never been studied.

Fortunately, the great mobility of the electrons along magnetic field lines suggests that in the real plasma the amplitude of the poloidal density variations and those of the selfconsistent potential are likely to be much smaller than predicted when mapping is performed ignoring the presence of the ambipolar potential. Accordingly, a 'zero-order' approximation has been implemented in SSFPQL, consisting of ignoring Φ altogether, but ensuring charge neutrality by replacing the missing ions reflected before reaching the IC resonance by the appropriate number of ions at the local temperature. In the absence of a rigorous approach to treating this effect, we are confident that this method provides a reasonably realistic solution to the problem.

5 Conclusions

The flexibility and the easy of use of the TORIC-SSFPQL codes has been illustrated with two different examples, obtained running the codes on a personal laptop computer. The first is the interpretation of the results of an IC heating experiment in a medium size tokamak; the second is the exploration of a proposed IC heating scenario in a future fusion grade plasma. Some new feature of the codes have been mentioned and used in the examples, in particular the inclusion of the effects of toroidal trapping in the evaluation of the QL diffusion coefficient by SSFPQL.

The most important element still missing for completely realistic simulations of IC heating experiments is a satisfactory model of radial diffusion and losses of the heated ions. This problem could be partially solved by coupling TORIC-SSFPQL to a transport code. While, however, in most such codes only a global, often partly empirical model of radial diffusion is implemented, it likely that the suprathermal, anisotropic populations produced by IC heating diffuse radially rather faster than the thermal plasma. In the present 'stand-alone' version, in SSFPQL radial diffusion losses are modelled as the interaction of the suprathermal ions with a thermal bath, implemented as a linearized Coulomb collisional operator with a Maxwellian background [11]. This model is acceptable if the radial diffusion is sufficiently slow compared to the collisional exchanges of the fast ions with the rest of the plasma, a situation which will prevail in large reactor-grade plasmas, but probably not in medium size tokamaks. As a consequence, it is likely that SSFPQL somewhat overestimates the energy content of the suprathermal populations produced by IC heating in present day experiments. To partially solve this problem, we have implemented a simple model of the ICRF power deposition broadening due to effects of the finite banana-width orbits [24]. This has been necessary to improve the agreement with Charge Exchange Recombination Spectroscopy on ^{3}He measurements [25].

References

[1] M. Brambilla, Numerical simulation of ion cyclotron waves in tokamak plasmas, Plasma Physics and Controlled Fusion **41**, 1 (1999). https://doi.org/10.1088/0741-3335/41/1/002

[2] M. Brambilla, Quasi-linear ion distribution function during ion cyclotron heating in tokamaks, Nuclear Fusion **34**, 1121 (1994). https://doi.org/10.1088/0029-5515/34/8/I06

[3] M. Brambilla, R. Bilato, Advances in numerical simulations of ion cyclotron heating of non-maxwellian plasmas, Nuclear Fusion **49**, 085004 (2009). https://doi.org/10.1088/0029-5515/49/8/085004

[4] J. Killeen, A.A. Mirin, M.E. Rensink, The solution of the kinetic equations for a multispecies plasma, **16**, 389 (1976). https://doi.org/10.1016/B978-0-12-460816-0.50016-6

[5] M. Brambilla, R. Bilato, An efficient interface between the solvers of maxwell's equations and of the quasilinear kinetic equation for simulations of ion cyclotron heating in tokamak plasmas, Computer Physics Communications **184**, 2053 (2013). http://doi.org/10.1016/j.cpc.2012.12.029

[6] M. Brambilla, Iterative solution of the Grad–Shafranov equation in symmetric magnetic coordinates, Physics of Plasmas **10**, 3674 (2003). https://doi.org/10.1063/1.1600736

[7] P.J. Catto, J.R. Myra, A quasilinear description for fast-wave minority heating permitting off-magnetic axis heating in a tokamak, Physics of Fluids B: Plasma Physics **4**, 187 (1992). https://doi.org/10.1063/1.860432

[8] R. Bilato, V. Belmondo, M. Brambilla, O. Maj, E. Poli, Progress on the ICRF orbit-averaged quasilinear operator of TORIC full-wave code, in *43rd EPS Conference on Plasma Physics* (2016), https://info.fusion.ciemat.es/OCS/eps2016pap/pdf/P1.045.pdf

[9] Y. Feng, B. Wolle, K. Hübner, New, simplified technique for calculating particle source rates due to neutral beam injection into tokamaks, Computer Physics Communications **88**, 161 (1995). http://doi.org/10.1016/0010-4655(95)00013-6

[10] R. Bilato, M. Brambilla, Y. Feng, G. Tardini, A neutral beam injection source for the TORIC/SSFPQL package, in *37th EPS Conference on Plasma Physics* (2010), https://info.fusion.ciemat.es/OCS/EPS2010PAP/pdf/P5.144.pdf

[11] R. Bilato, M. Brambilla, O. Maj, L. Horton, C. Maggi, J. Stober, Simulations of combined neutral beam injection and ion cyclotron heating with the TORIC-SSFPQL package, Nuclear Fusion **51**, 103034 (2011). https://doi.org/10.1088/0029-5515/51/10/103034

[12] R. Bilato, M. Brambilla, E. Poli, On the approximations of the distribution function of fusion alpha particles, Physics of Plasmas **21**, 104502 (2014). http://doi.org/10.1063/1.4897323

[13] R. Bilato, M. Brambilla, E. Fable, Simulations of fast-wave current drive in pulsed and steady-state DEMO designs, Journal of Physics: Conference Series **561**, 012001 (2014). https://doi.org/10.1088/1742-6596/561/1/012001

[14] M. Brambilla, R. Bilato, On radio frequency current drive in the ion cyclotron range of frequencies in DEMO and large ignited plasmas, Nuclear Fusion **55**, 023016 (2015). https://doi.org/10.1088/0029-5515/55/2/023016

[15] M. Brambilla, Finite larmor radius wave equations in tokamak plasmas in the ion cyclotron frequency range, Plasma Physics and Controlled Fusion **31**, 723 (1989). https://doi.org/10.1088/0741-3335/31/5/004

[16] R. Bilato, M. Brambilla, Z. Jiang, Implementing zero-banana-width quasilinear operator for fast icrf simulations, Journal of Physics: Conference Series **401**, 012001 (2012). https://doi.org/10.1088/1742-6596/401/1/012001

[17] R. Bilato, T. Odstrcil, F. Casson, C. Angioni, M. Brambilla, Y. Kazakov, E. Poli, The impact of the ion-cyclotron-resonance location on the poloidal asymmetries of impurity density in an ICRF-heated rotating plasma, Nuclear Fusion **57**, 056020 (2017). https://doi.org/10.1088/1741-4326/aa5fd6

[18] V. Bobkov, R. Bilato, L. Colas, R. Dux, E. Faudot, H. Faugel, H. Fünfgelder, A. Herrmann, J. Jacquot, A. Kallenbach et al., Characterization of 3-strap antennas in ASDEX Upgrade, EPJ Web Conf. **157**, 03005 (2017). https://doi.org/10.1051/epjconf/201715703005

[19] R. Bilato, O. Maj, M. Brambilla, An algorithm for fast Hilbert transform of real functions, Advances in Computational Mathematics **40**, 1159 (2014). http://doi.org/10.1007/s10444-014-9345-4

[20] R. Bilato, N. Bertelli, M. Brambilla, R. Dumont, E.F. Jaeger, T. Johnson, E. Lerche, O. Sauter, D. Van Eester, L. Villard, Status of the benchmark activity of ICRF full-wave codes within EUROfusion WPCD and beyond, AIP Conference Proceedings **1689**, 060001 (2015). http://doi.org/10.1063/1.4936499

[21] A. Messiaen, R. Koch, R. Weynants, P. Dumortier, F. Louche, R. Maggiora, D. Milanesio, Performance of the ITER ICRH system as expected from TOPICA and ANTITER II modelling, Nuclear Fusion **50**, 025026 (2010). https://doi.org/10.1088/0029-5515/50/2/025026

[22] V. Belmondo, R. Bilato, M. Brambilla, O. Maj, Orbit-averaged quasilinear diffusion operator in the ion-cyclotron range of frequencies, Journal of Physics: Conference Series **260**, 012001 (2010). https://doi.org/10.1088/1742-6596/260/1/012001

[23] R. Bilato, O. Maj, C. Angioni, Modelling the influence of temperature anisotropies on poloidal asymmetries of density in the core of rotating plasmas, Nuclear Fusion **54**, 072003 (2014). https://doi.org/10.1088/0029-5515/54/7/072003

[24] R. Bilato, M. Brambilla, Multi-frequency ICRF simulations of NBI-heated plasmas with TORIC-SSFPQL package, 49th EPS Conference on Plasma Physics (2023).

[25] A. Kappatou, M. Weiland, R. Bilato, Y. Kazakov, R. Dux, V. Bobkov, T. Pütterich, R. McDermott, the EUROfusion MST1 team, the ASDEX Upgrade team, CXRS measurements of energetic helium ions in ASDEX upgrade plasmas heated with a 3-ion ICRF scenario, Nuclear Fusion **61**, 036017 (2021). https://doi.org/10.1088/1741-4326/abca57